THE JOURNAL OF PHYSICAL CHEMISTRY B

Article

pubs.acs.org/JPCB

Curcumin in Reverse Micelle: An Example to Control Excited-State Intramolecular Proton Transfer (ESIPT) in Confined Media

Chiranjib Banerjee, Chiranjib Ghatak, Sarthak Mandal, Surajit Ghosh, Jagannath Kuchlyan, and Nilmoni Sarkar*

Department of Chemistry, Indian Institute of Technology, Kharagpur 721302, WB, India

Supporting Information

ABSTRACT: In this Article, we focused on the modulation of the photophysical properties of curcumin, an anti-cancer drug, in aqueous and nonaqueous reverse micelles of AOT in *n*-heptane using steady-state and time-resolved fluorescence spectroscopy. The instability of curcumin is a common problem which restricts its numerous applications like Alzheimer disease, HIV infections, cystic fibrosis, etc. Our study reveals that curcumin shows comparatively higher stability after encapsulation into the interfacial region of the reverse micelle. To get a vivid description of the micro-environment, we added hydrogen-bond-donor (HBD) as well as non-hydrogen-bond-donor (NBD) core solvents. For experimental purposes, we used water, ethylene glycol (EG), glycerol (GY) as HBD solvents and *N*,*N*-dimethyl formamide (DMF) as a NBD solvent. With increasing amount of core solvents, irrespective of HBD or NBD, the fluorescence intensity and lifetime of curcumin increase with remarkable red-shift inside the reverse micelle. This is attributed to the modulation of the nonradiative rates associated with the excited-state intermolecular hydrogen bonding between the pigment and the polar solvents. We obtained a high partition constant at $W_0 = 0$ (W_0 = [core solvent]/[AOT]) which is certainly due to the hydrogen bonding between the negatively charged sulfonate group of AOT and hydroxyl groups of curcumin. Steady-state anisotropy and time-resolved results give an idea about the microenvironment sensed by the curcumin molecules. The red-shift of emission spectra, increase in the value of $E_T(30)$, as well as the increase in the fluorescence lifetime were interpreted as being caused by the partition of the probe between the micellar interface and the polar core solvent. Indeed, we show here that it is possible to control the excited state intramolecular proton transfer (ESIPT) process of curcumin by simply changing the properties of the AOT reverse micelle interfaces by choosing the appropriate polar solvents to make the reverse micelle media.

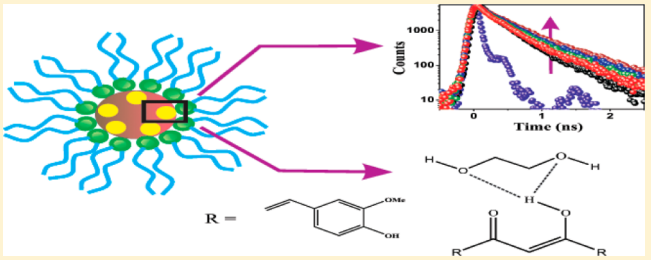

1. INTRODUCTION

Curcumin is a natural yellow orange pigment derived from the rhizome of the plant *Curcuma longa* L., popularly called turmeric, a member of the Zingiberaceae family. It has been extensively used as a spice, food preservative, and coloring agent.[1] As a nontoxic and highly promising natural antioxidant compound having a wide range of biological applications, it is anticipated that curcumin may in the near future find applications as a novel drug to control various diseases, including inflammatory disorders, carcinogenesis, and oxidative stress-induced pathogenesis.[2−4] Moreover, curcumin can inhibit the metabolic action of aflatoxin B1,[5] aminopeptidase N,[6] lipoxygenase,[7] cycloxygenase,[8] ornithine decarboxylase,[9] and the efflux transporters MRP1 and MPR2.[10] Finally, it appears to have a potential in the treatment of Alzheimer disease[11] and cystic fibrosis,[12] as well as being considered a drug or model substance for the treatment of HIV infections[13−15] and as an immune-stimulating agent.[13] Studies on curcumin showed that it is safe even at high doses of 12 g/day[16,17] in animal and human trials, but its effectiveness is limited by low solubility and poor bioavailability in aqueous medium. Several studies like measurement of blood plasma levels and biliary excretion showed that curcumin was poorly absorbed from the gut and the quantity of curcumin that reached the tissues outside the gut was pharmacologically insignificant. The studies indicated the insolubility of curcumin in water at physiological pH, limited absorption, poor bioavailability, rapid metabolism, and excretion.[18] The instability of curcumin at physiological pH may be due to the β-diketone linker in the seven carbon chain of curcumin. Therefore, the improvement in stability, solubility, and bioactivity of curcumin is needed. As a consequence, there are significant interests in developing a detailed level of understanding of the photophysical and photochemical processes of curcumin in order to further exploit its potential medicinal effects.

Curcumin is highly soluble in polar organic compounds but is only slightly soluble in aliphatic or alicyclic organic solvents such as hexane and cyclohexane. As shown in Scheme 1, the systematic name of curcumin, 1,7-bis(4-hydroxy-3-methoxy-phenyl)-1,6-hepatadiene-3,5-dione, suggests that curcumin is a

Received: February 21, 2013
Revised: April 17, 2013

   dx.doi.org/10.1021/jp401840z | *J. Phys. Chem. B* XXXX, XXX, XXX−XXX

Scheme 1. Structures of Curcumin and AOT

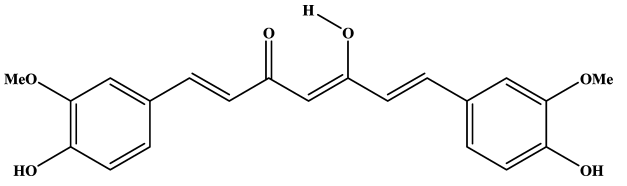

Curcumin

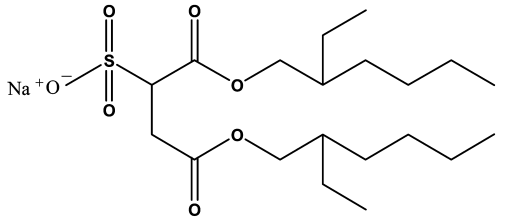

Aerosol-OT (AOT)

α-diketone tautomer. However, X-ray crystal structure analysis has established that curcumin and its bisacetoxy derivative can exist as a keto−enol form.[19,20] The ^{1}H and ^{13}C NMR studies also confirmed the presence of the enol form in nonpolar, polar, and protic solvents.[21] Recently, Huppert and co-workers studied the temperature dependent fluorescence property of curcumin in various organic solvents and showed that nonradiative rate constants at temperatures of 175−250 K follow the same trend as the dielectric relaxation time of the respective solvents. They attributed the nonradiative process to solvent controlled proton transfer.[22] The same group also studied the effect of mild base on curcumin in organic solvent and more interestingly have found that the average fluorescence decay time is reduced in the presence of sodium acetate, as a weak base, due to the excited-state proton transfer (ESPT) from the acidic groups of curcumin to the acetate anion.[23]

Several methods have been developed to address the issue of low solubility and stability of curcumin. Encapsulation in polymeric nanoparticles; aggregation of cross-link and random copolymers, has shown promise as a good stabilizer as well as a potentially effective method for delivering curcumin.[24] Petrich and co-workers showed that aggregation of surfactants, including sodium dodecyl sulfate (SDS), cetyl trimethylammonium bromide (CTAB), and Triton X-100, into micelles also provided desirable effects in solubilizing and stabilizing curcumin.[25] Kee and co-workers studied the curcumin in cationic micelles and showed that cationic micelles are capable of stabilizing curcumin at elevated pH, which is the condition often used in the studies of curcumin's medicinal effects.[26] Several groups also reported that curcumin can be stabilized in lipid bilayers and vesicles as a delivery system for administration of curcumin as a drug.[27,28] More recently, the use of serum albumin as a stabilizer for curcumin has also been reported in the literature.[29]

Many important biological reactions and fundamental processes take place at interfaces like membranes, which provide a constrained environment where the properties of the solvents change in a drastic manner. Various studies show that the structure of the solvents at interfaces is different from that in the bulk;[30−32] hence, the understanding of photophysical properties of curcumin in these organized assemblies is essential for the better understanding of its medicinal effect.

In the last few decades, a lot of studies have been performed to reveal the structure as well as the biological importance of the confined water in the reverse micelle pool.[33,34] Pileni et al. showed that the size of the reverse micelle can be controlled by different techniques and described their probable reasons.[33−35] In recent years, attempts have been made to prepare and study waterless reverse micelles where water has been replaced by polar solvents, which have relatively high dielectric constants and are immiscible in hydrocarbon solvents. These nonaqueous microemulsion systems are superior to the aqueous ones particularly because they can be used as good reaction media. They are, of course, especially attractive for those reactants that may react with water.[36] Despite their potential use, the literature on these waterless microemulsions is scarce. The most common polar solvents used include formamide (FA), dimethylformamide (DMF), dimethylacetamide (DMA), ethylene glycol (EG), propylene glycol (PG), and glycerol (GY). Sodium bis(2-ethylhexyl) sulfosuccinate (Aerosol-OT, AOT) or Docusate sodium is the most commonly used surfactant for reverse micelle preparation.[37] In this Article, we investigate the excited state properties of curcumin inside several types of AOT-reverse micelles by using different core solvents such as water, EG, GY, and DMF with variation of W_0 values (W_0 = [core solvent]/[AOT]). The fundamental aim in this present Article is to reveal the photophysical properties of curcumin such an environment having unique properties regarding polarity, rigidity, morphology, etc. Besides this, we have tried to explore the fate of the excited state intramolecular proton transfer (ESIPT) process inside reverse micelles. Finally, we have shown that a more rigid and confined environment inside the reverse micelle is a better model to control the ESIPT process of curcumin.

2. EXPERIMENTAL SECTION

2.1. Materials. AOT (Sigma-Aldrich) was dried over 24 h with a high energy vacuum pump. All the solvents used were purchased from Spectrochem (spectroscopic grade) and used as received. Curcumin obtained from Sigma-Aldrich (purity ∼81%) was purified by the column chromatographic technique, and the purity of the sample used (∼99%) was checked by the HPLC technique.[38] The structures of the AOT and curcumin are given in Scheme 1. Milli-Q water was used to prepare all solutions. The concentration of curcumin in all the experiments was kept at 2.5×10^{-6} M.

2.2. Instruments and Methods. The absorption and fluorescence spectra were recorded using a Shimadzu (model no. UV-2450) spectrophotometer and Hitachi (model no. F-7000) spectrofluorimeter. All the fluorescence emission spectra and steady-state anisotropy at a particular wavelength were corrected for the wavelength sensitivity of the detection system. Steady-state anisotropy is defined as[39]

$$r_0 = \frac{I_{VV} - G \cdot I_{VH}}{I_{VV} + 2G \cdot I_{VH}} \quad (1)$$

where G is the correction factor. I_{VV} and I_{VH} are fluorescence decays for polarized parallel and perpendicular to the polarization of the excitation light, respectively. Fluorescence lifetimes were obtained from a time-correlated single photon counting (TCSPC) spectrometer using nano-LED (IBH, U.K.) as the light source at 408 nm. The experimental setup for picosecond TCSPC has been described elsewhere.[40] Briefly, the samples were excited at 408 nm using a picosecond laser diode

dx.doi.org/10.1021/jp401840z | J. Phys. Chem. B XXXX, XXX, XXX−XXX

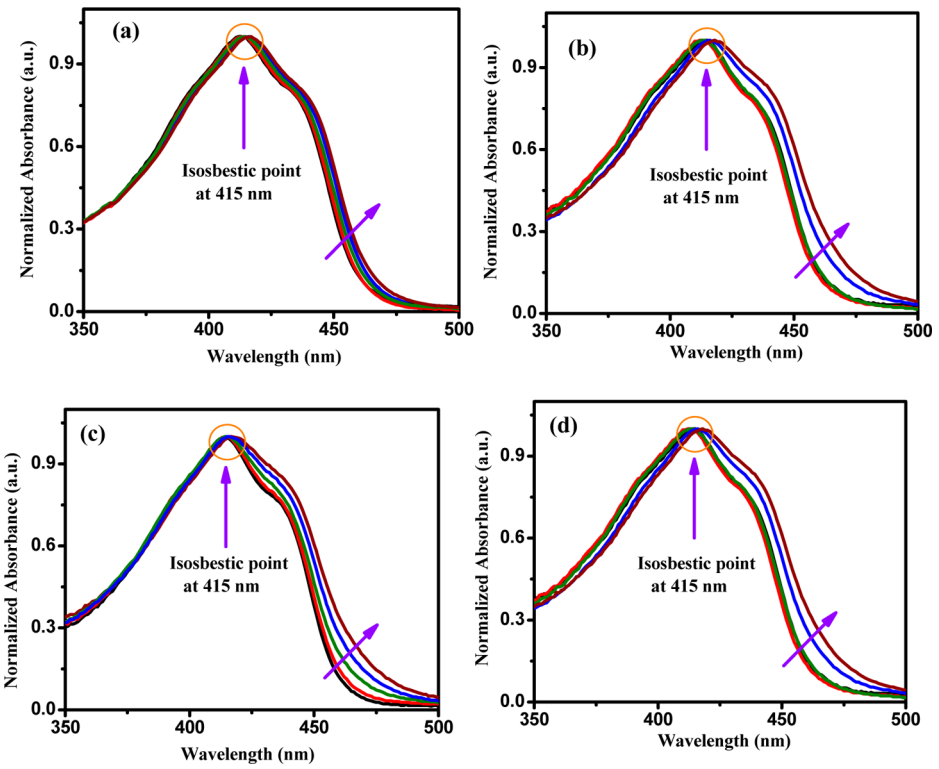

Figure 1. Absorption spectra of curcumin at W_0 = 0.0, 0.5, 1.0, 1.5, and 2.0 for (a) water/AOT reverse micelle, (b) EG/AOT reverse micelle, (c) GY/AOT reverse micelle, and (d) DMF/AOT reverse micelle.

(IBH, Nanoled), and the signals were collected at the magic angle (54.7°) using a Hamamatsu microchannel plate photomultiplier tube (3809U). The instrument response function of our setup was 90 ps.

The average fluorescence lifetimes for the decay curves were calculated from the decay times and the relative contributions of the components using the following equation[39]

$$\langle \tau \rangle = a_1\tau_1 + a_2\tau_2 \quad (2)$$

where τ_1 and τ_2 are the first and second components of the decay time of curcumin and a_1 and a_2 are the corresponding relative amplitudes of these components.

We have calculated the quantum yield of curcumin by the following equation:[39]

$$\frac{\Phi_S}{\Phi_R} = \frac{A_S}{A_R} \times \frac{(\mathrm{Abs})_R}{(\mathrm{Abs})_S} \times \frac{{n_S}^2}{{n_R}^2} \quad (3)$$

where Φ represents the quantum yield, Abs represents the absorbance, A represents the area under the fluorescence curve, and n is the refractive index of the medium. The subscripts S and R denote the corresponding parameters for the sample and reference, respectively. Rhodamin 6G was taken as the standard solution.

3. RESULTS AND DISCUSSION

3.1. Steady-State Absorption and Emission Studies. Absorption and emission spectra of curcumin were measured in bulk *n*-heptane, water, EG, DMF, and GY solvents and inside AOT reverse micelles. Curcumin shows absorption maxima in *n*-heptane at 408 nm/430 nm which are different from the absorption maxima obtained for reverse micellar solution (Figure S1, Supporting Information). In reverse micellar solution, we obtained absorption maximum of curcumin at 415 nm with a shoulder at ~436 nm, at W_0 = 0.0 and gradually shifted toward the red-end side in the same fashion with increasing W_0, irrespective of the nature of the different core solvents used in this study (Figure 1). This trend indicates the nature of the interaction between the curcumin and different core solvents is quite the same in AOT reverse micelle as all the core solvents are able to form a similar type of hydrogen bonding with curcumin. (It is important to note that DMF is unable to engage in N—H···O═C hydrogen bonding with dialkyl substitution at nitrogen. However, it can form C—H···O and C═O···H type hydrogen bonds.) Again, the absorption peaks in water, EG, DMF, and GY occur at 431/350, 435, 450/428, and 438 nm, respectively, which are quite different compared with their reverse micellar solutions (these individual spectra are not shown here). Such results help us to understand the introduction of a new microenvironment around the drug inside reverse micellar solutions. Since the normalized absorption spectra of curcumin in the AOT reverse micelles with water, EG, DMF, and GY as a function of W_0 show neat isosbestic points at 415 nm, the equilibrium of the probe between the two microenvironments can be realized. The red-shifted absorption spectra with fair increment of the shoulder at the red-end with increase in W_0 confirm the transfer of curcumin from the bulk *n*-heptane phase to a more polar environment. To find the location of the probe, we have constructed the difference in absorption spectra of curcumin in *n*-hexane without AOT and with AOT and core solvents (at various W_0). The difference in the absorbance spectra of curcumin in *n*-heptane with AOT and gradual addition of core solvents exhibits a negative absorbance around 385 nm, and there is a distinct peak at 444 nm. The depletion of the population of curcumin in *n*-heptane on addition of polar core solvents can be realized by increasing the negative absorbance

dx.doi.org/10.1021/jp401840z | J. Phys. Chem. B XXXX, XXX, XXX−XXX

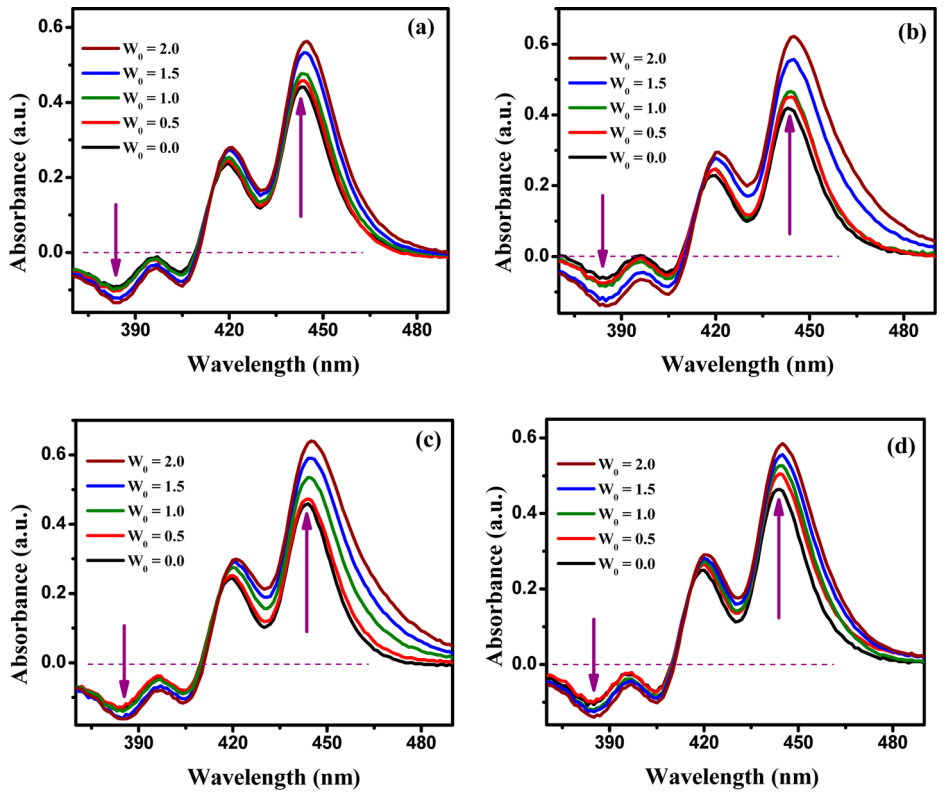

Figure 2. Difference absorption spectra of curcumin at W_0 = 0.0, 0.5, 1.0, 1.5, and 2.0 for (a) water/AOT reverse micelle, (b) EG/AOT reverse micelle, (c) GY/AOT reverse micelle, and (d) DMF/AOT reverse micelle.

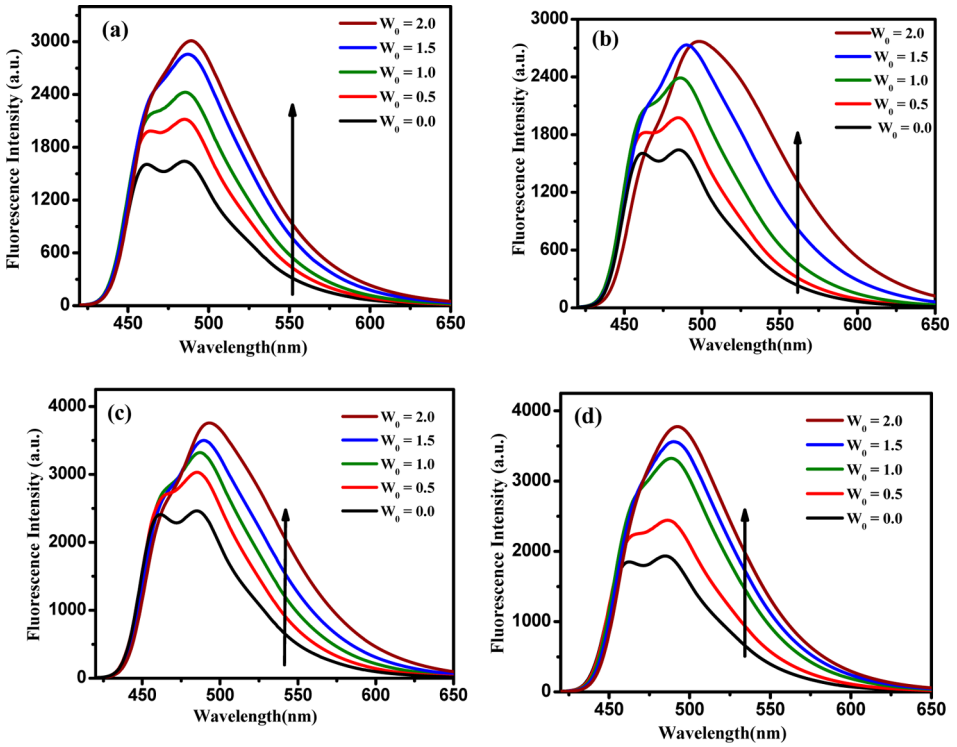

Figure 3. Emission spectra (λ_{ex} = 408 nm) of curcumin at W_0 = 0.0, 0.5, 1.0, 1.5, and 2.0 for (a) water/AOT reverse micelle, (b) EG/AOT reverse micelle, (c) GY/AOT reverse micelle, and (d) DMF/AOT reverse micelle.

value at 385 nm. On the other hand, the increase of optical density at 444 nm indicates that the probe molecules are shifted toward the polar region of the microemulsions. The representative difference in absorbance spectra of curcumin in AOT reverse micelle is given in Figure 2. The increase in absorbance after gradual addition of core solvent also supports the preferential solubility of the drug inside the reverse micellar phase.

dx.doi.org/10.1021/jp401840z | J. Phys. Chem. B XXXX, XXX, XXX−XXX

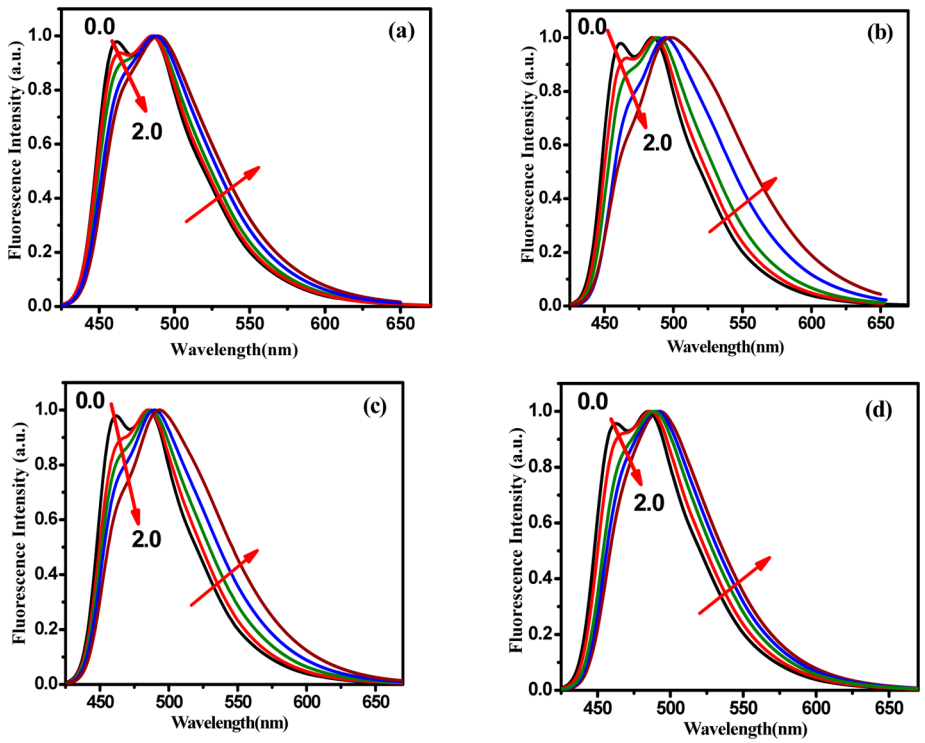

Figure 4. Normalized emission spectra (λ_{ex} = 408 nm) of curcumin at W_0 = 0.0, 0.5, 1.0, 1.5, and 2.0 for (a) water/AOT reverse micelle, (b) EG/AOT reverse micelle, (c) GY/AOT reverse micelle, and (d) DMF/AOT reverse micelle.

Although curcumin is barely soluble in water, its solubility is considerably increased in the presence of reverse micellar solution. However, in other core solvents (EG, DMF, GY), the solubility of curcumin is considerably high. Thus, from the beginning, we had to consider the fact of partial abundance of curcumin in the bulk *n*-heptane along with a large distribution over the reverse micellar phase. We have taken emission spectra of the curcumin in all the core solvents and in *n*-heptane. Curcumin shows emission maxima at 556 nm in EG, 528 nm in DMF, 545 nm in GY, and in *n*-heptane, it shows three maxima at 442, 470, and 502 nm, respectively. As we are aware, curcumin shows a high sensitivity to the solvent polarity, so the difference is due to the different polarities of the core solvents. The most striking observations regarding the emission spectra of curcumin inside all the reverse micellar solutions are as follows. In all cases, we obtained similar types of emission spectra, in which the amount of increase of the low energy band (485 nm) is quite large compared to the amount of increase in the high energy band (461 nm). The emission peak maxima with variation of W_0 for various reverse micelles are listed in Table S1 (Supporting Information). From Figure 3, we can observe two emission peaks at 461 and 485 nm at W_0 = 0 for all the reverse micelles and a gradual increase in emission intensity with considerable red-shift with the addition of core solvents. The contribution of a high energy emission band (461 nm) gradually vanishes, which implies that the percentage of curcumin in bulk *n*-heptane gradually decreases with addition of various core solvents. In all cases, the amount of red-shift of the high energy emission band is negligible, ∼2 nm, but for the low energy emission band (485 nm), it has a considerable value of ∼9−13 nm. The difference between the emission spectra of curcumin inside various reverse micelles depends upon the hydrogen-bond-donor capabilities of the polar core solvents. In the case of water/AOT reverse micelles, the amount of red-shift is quite small, ∼5 nm, compared to that for other reverse micelles; this is due to the presence of water in the pool of reverse micelles, which is a nonpreferable solvent for curcumin. Such differences with the other reverse micelles can also be clearly observed from Figure 4. The increase in the shoulder height at the red-end side of the normalized emission spectra for all the reverse micelles is quite high compared with water/AOT reverse micelles. Such an increment in shoulder height with increase in polar core solvent again indicates the preferential transfer of curcumin toward the reverse micellar phase from bulk *n*-heptane. One can also compare the steady-state result by considering the Kamlet−Taft parameters of the used solvents (listed in Table S2, Supporting Information). From the Kamlet−Taft scale, it is evident that both EG and GY are good HBD solvents; hence, there is a strong possibility of intermolecular hydrogen bond formation between curcumin and EG/GY. The HBD ability of water is also high, although, due to the instability of curcumin in water, the red-shift of the emission peak is small compared to other core solvents. Curcumin (presence of both keto−enol groups) may also form a hydrogen bond with DMF due to its high hydrogen-bond-accepting ability.

From close inspection of UV−visible and fluorescence results, we can presumably ascertain that curcumin is preferably located in such a region which is a common feature for all the reverse micelles, i.e., the interfacial region at W_0 = 0. The interfacial region is such a region which has higher polarity than that of the bulk dispersing solvent but lower than the polar core solvent. The hydrogen bonding between the negatively charged sulfonate group of AOT and free hydroxyl groups of curcumin may be the reason for such observation. Moreover, hydrophobic interaction between the big drug molecules with the nonpolar moiety just immediate to the headgroup of AOT may also play a crucial role. In the case of core solvents, which have

dx.doi.org/10.1021/jp401840z | J. Phys. Chem. B XXXX, XXX, XXX−XXX

the capability to form hydrogen bonding (hydrogen-bond-donating solvents) like water, EG and GY, structured interfacial regions are available due to the presence of hydrogen bonding, but for a solvent like DMF, which is unable to form a hydrogen bond (not able to donate a hydrogen bond), the interfacial regions are less structured. It is well-known that alcohols form a hydrogen bonding complex with AOT between the hydroxyl groups of alcohols and the ionic head of the AOT.[41] Moreover, various studies have shown that the formation of solvated reverse micelles is absolutely associated with the ability to form a large number of hydrogen bonds of the encapsulated polar solvents.[36,42] The presence of a clear isosbestic point with gradual addition of core solvent is a manifestation of the presence of curcumin in two different environments.

It is also known that the interactions of AOT with hydrogen-bond-donor solvents follow the order GY > EG > water. In that sense, it is probably true that, when GY is the polar sequestered solvent, the AOT reverse micelle interface is highly structured compared to the other two solvents. In the case of DMF, the interface of reverse micelle is less structured which may be rationalized by the noninteracting nature of DMF with AOT through hydrogen bonding. As a consequence, one can conclude that curcumin faced a less structured environment when non-hydrogen-bond-donor solvents are used as a core solvent and it faced a more structured environment when hydrogen-bond-donor solvents are being used. However, most interestingly, our steady-state results suggest that with the addition of polar core solvents the transfer of curcumin has occurred from the reverse micelle interface to the polar core irrespective of their hydrogen bonding ability with AOT. This may be due to the formation of an intermolecular hydrogen bond between the keto−enol group of curcumin and core solvents. Our time-resolved data also support this phenomenon (vide infra).

3.2. Measurement of Polarity of the Microenvironment. The measurement of the fluorescence Stokes shift of a probe molecule is a very useful technique to measure reorganization of the probe's local environment. Herein, we observed that curcumin shows a Stokes shift of 3475 cm^{-1} in an AOT/*n*-heptane reverse micelle aggregate at $W_0 = 0$ (Table 1).

Table 1. $E_T(30)$ Values versus Stokes Shifts of Curcumin with Variation of W_0

system	W_0	$E_T(30)$	Stokes shift (cm^{-1})
water/AOT	0	42.19	3475
	0.5	42.44	3512
	1.0	42.77	3565
	1.5	43.08	3608
	2.0	43.59	3683
EG/AOT	0.5	43.03	3608
	1.0	43.59	3682
	1.5	44.43	3814
	2.0	45.78	4005
GY/AOT	0.5	42.56	3538
	1.0	43.07	3613
	1.5	43.59	3693
	2.0	44.45	3810
DMF/AOT	0.5	42.68	3561
	1.0	43.20	3633
	1.5	43.90	3744
	2.0	44.47	3822

However, with addition of polar solvents, it shifts to a higher value, which is an indication of the gradual movement of curcumin from the reverse micelle interface to its polar core. For a better understanding of the polarity of the microenvironment, we measured the $E_T(30)$ values with various W_0. To determine the $E_T(30)$ values, we plotted the Stokes shift versus $E_T(30)$ of a series of alcohols (C_nOH, where n = 1, 2, 3, 4, 5, 6, 8) as a reference scale (Figure S2, Supporting Information).[43] The calculation of $E_T(30)$ values confirms that curcumin locates in different zones of the AOT reverse micelle that differ in their micropolarities. The highest polarity region that curcumin exists when EG is encapsulated; $E_T(30)$ value changes from 42.19 to 45.78 at $W_0 = 0$ to $W_0 = 2.0$, while curcumin faces intermediate polarity in the case of GY/AOT and DMF/AOT reverse micelle and the $E_T(30)$ value changes to 44.45 and 44.47 at $W_0 = 2.0$. However, in the case of water/AOT reverse micelle, curcumin faces the least polarity region; the $E_T(30)$ value changes to 43.59 at $W_0 = 2.0$. The increment in fluorescence intensity with increase in $E_T(30)$ value upon addition of polar solvents clearly proves that curcumin undergoes a favorable transfer from the interfacial region of a reverse micelle to its core. The strong red-shift in emission spectra with considerable increase in quantum yield (0.051) with addition of polar solvents clearly indicates that the polarity around the drug increases. The variation of quantum yield with $E_T(30)$ values is shown in Figure S3 (Supporting Information).

3.3. Determination of Partition Constant. To evaluate the partition constant between curcumin and AOT/*n*-heptane primary aggregates, the pseudophase model has been applied.[44−46] In this model, the reverse micelle should be considered as a distinct pseudophase, whose properties are independent of AOT concentration and are only determined by the value of the characteristic parameter W_0. This model also considers two solubilizing sides which are the external solvents and the reverse micelle interface (i.e., all the surfactant molecules). In this way, the distribution of curcumin between the micelle and the external solvent defined in eq 4 can be expressed in terms of the partition constant (K_p) shown in eq 5.

$$\text{curcumin}_f \rightleftharpoons \text{curcumin}_b^l \tag{4}$$

$$K_p = \frac{[\text{curcumin}]_b^l}{[\text{curcumin}]_f} \tag{5}$$

The subscripts "f" and "b" denote the free and bound curcumin in terms of local concentrations (superscript "l"). Now, if $[\text{curcumin}]_b$ is the analytical (bulk) concentration of micelle bound substrate, eq 6 can be deduced.

$$[\text{curcumin}]_b^l = \frac{[\text{curcumin}]_b}{[\text{AOT}]} \tag{6}$$

Hence, one can express the distribution of curcumin between AOT and *n*-heptane in terms of the partition constant (K_p) shown in eq 7.

$$K_p = \frac{[\text{curcumin}]_b}{[\text{curcumin}]_f[\text{AOT}]} \tag{7}$$

where $[\text{curcumin}]_b$ is the analytical concentration of the substrate incorporated into the reverse micelle, $[\text{curcumin}]_f$ is the concentration of the substrate in the organic solvent, and [AOT] is the micellized surfactant (total AOT concentration minus the operational CMC i.e., 10^{-4}). This equation is

dx.doi.org/10.1021/jp401840z | J. Phys. Chem. B XXXX, XXX, XXX−XXX

applicable at a fixed W when the analytical concentration of probe ≪ [AOT].

The value of K_p can be determined from the change in the fluorescence intensity of the probe with the surfactant concentration measured at a given wavelength. If the analytical concentration of the probe is kept constant and the absorbance of the sample at the working excitation wavelength is low,[47,48] eq 8 can be deduced:

$$I = \frac{I_0(\phi_f + \phi_b K_p[\mathrm{AOT}])}{(1 + K_p[\mathrm{AOT}])} \quad (8)$$

where I_0 is the intensity of incident light, I_f and I_b are the fluorescent intensities when the probe is present in the external solvent and in the disperse pseudophase, respectively, I is the fluorescence intensity measured at the surfactant concentration considered, ϕ_f and ϕ_b are the fluorescent quantum yields of curcumin in the organic solvent and bound to the reverse micelle interface, respectively. The measured value for the partition constant (K_p) at W_0 = 0 was 30.07, which is little higher compared with other reported values. The high value of K_p can be realized by considering the hydrogen bonding between the negatively charged sulfonate group of AOT and the free hydroxyl groups of curcumin. The plot for the determination of partition constant is shown in Figure 5.

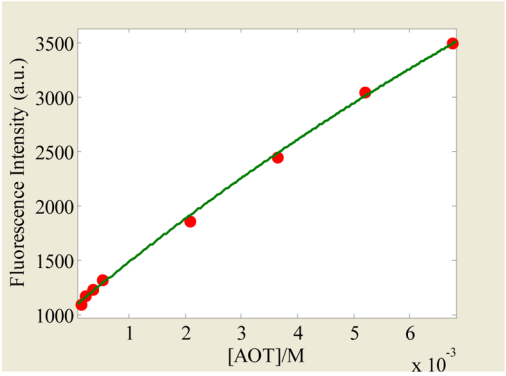

Figure 5. Plot of fluorescence intensity versus [AOT], for determination of partition function at W_0 = 0.

3.4. Steady-State Fluorescence Anisotropy Studies. We measured the steady-state fluorescence anisotropies (r_0) with variation at W_0 of various reverse micelle aggregates to get an idea about the rigidity of the microenvironment surrounding the fluorophore. Plots of anisotropy values with variation of W_0 for different reverse micelles are depicted in Figure 6, and the values are listed in Table 2. The steady-state anisotropy value of curcumin in AOT/*n*-heptane reverse micelle at W_0 = 0 is 0.2966. However, with an increase in W_0, it changes to certain values depending mainly on three major factors: One is the increase in polarity of the medium, another is the increase or decrease in microviscosity of the reverse micellar core, and the last one is the constraint of the local environment around the curcumin. The steady-state anisotropy value of curcumin in the water/AOT reverse micellar system changes from 0.2778 at W_0 = 0.5 to 0.2714 at W_0 = 2.0; i.e., there are very small changes around the microenvironment of the probe molecules with gradual addition of water. This can be explained by considering the two opposite factors, decrease the microviscosity around the probe molecules (responsible for reducing the anisotropy value) and increase the hydrogen bonding ability between curcumin and water (responsible for increasing the anisotropy value). As a result, the anisotropy value of curcumin remains almost constant. In the case of EG/AOT reverse micelle, a little increment has been observed; it changes from 0.2825 at W_0 = 0.5 to 0.3099 at W_0 = 2.0, which is an indication of the increase in restriction around the probe molecules due to the formation of hydrogen bonding between the carbonyl moiety of the curcumin and the hydroxyl moiety of the EG. A similar effect is also observed when GY is sequestered by AOT reverse micelle; it increased from 0.2765 at W_0 = 0.5 to 0.3046 at W_0 = 2.0. These changes can also be explained by assigning the hydrogen bond between the curcumin and GY. In the case of DMF/AOT reverse micelle, the anisotropy value gradually decreases from 0.2578 at W_0 = 0.5 to 0.2089 at W_0 = 2.0, which clearly follows the viscosity trend; i.e., with the gradual addition of the DMF, the size of the reverse micelle increases and at the same time the microviscosity of the reverse micellar core decreases; as a result, the anisotropy value decreases.

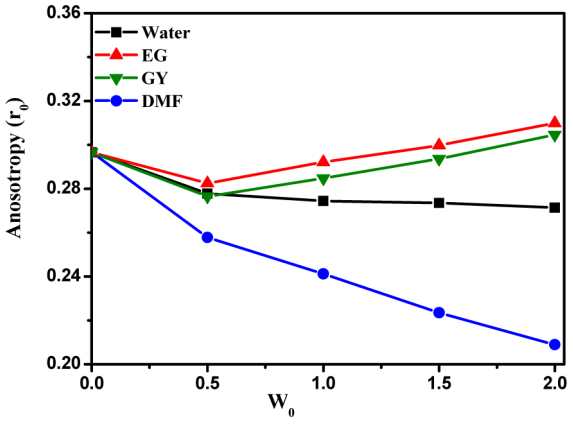

Figure 6. Plots of steady-state anisotropies of curcumin vs W_0 for various reverse micelles.

3.5. Time-Resolved Studies. The time-resolved fluorescence decays of curcumin in AOT/*n*-heptane primary aggregates as well as with addition of different core solvents were recorded at emission wavelengths of 461 and 485 nm with an excitation wavelength of 408 nm. The representative time-resolved fluorescence decay profiles of curcumin in the above-mentioned cases at 485 nm are depicted in Figure 7, and the corresponding lifetime values obtained from the biexponential fitting of the decays are given in Table 3. The fluorescence lifetime measurements provide the information about the location of the probe when there is an option of partitioning the probe between homogeneous and heterogeneous phases. The lifetime values of the probe, confined in the micellar environment, are significantly longer than those observed in pure homogeneous solvents. Unlike the steady-state fluorescence measurements, there are very few reports on the fluorescence lifetimes of curcumin. Therefore, it is also necessary to measure the lifetime in such biologically important microheterogeneous systems. The competing nonradiative processes shortened the fluorescence lifetimes considerably. The fluorescence decay profiles obtained from time correlated single photon counting (TCSPC) studies in most of the organized media as well as organic solvents showed a multiexponential fit, and the fluorescence lifetime values as well as their relative amplitudes varied significantly with the nature of the media.[43,49−51] Due to the complex nature, in most

dx.doi.org/10.1021/jp401840z | J. Phys. Chem. B XXXX, XXX, XXX−XXX

Table 2. Steady-State Anisotropy Values of Curcumin in Different Systems with Variation of W_0

	r_0[a]				
system	(W_0 = 0)	(W_0 = 0.5)	(W_0 = 1.00)	(W_0 = 1.5)	(W_0 = 2.0)
water/AOT	0.2966	0.2778	0.2744	0.2735	0.2714
EG/AOT	0.2966	0.2825	0.2921	0.2998	0.3099
GY/AOT	0.2966	0.2765	0.2848	0.2937	0.3046
DMF/AOT	0.2966	0.2578	0.2412	0.2235	0.2089

[a]Error in experimental data of ±3%.

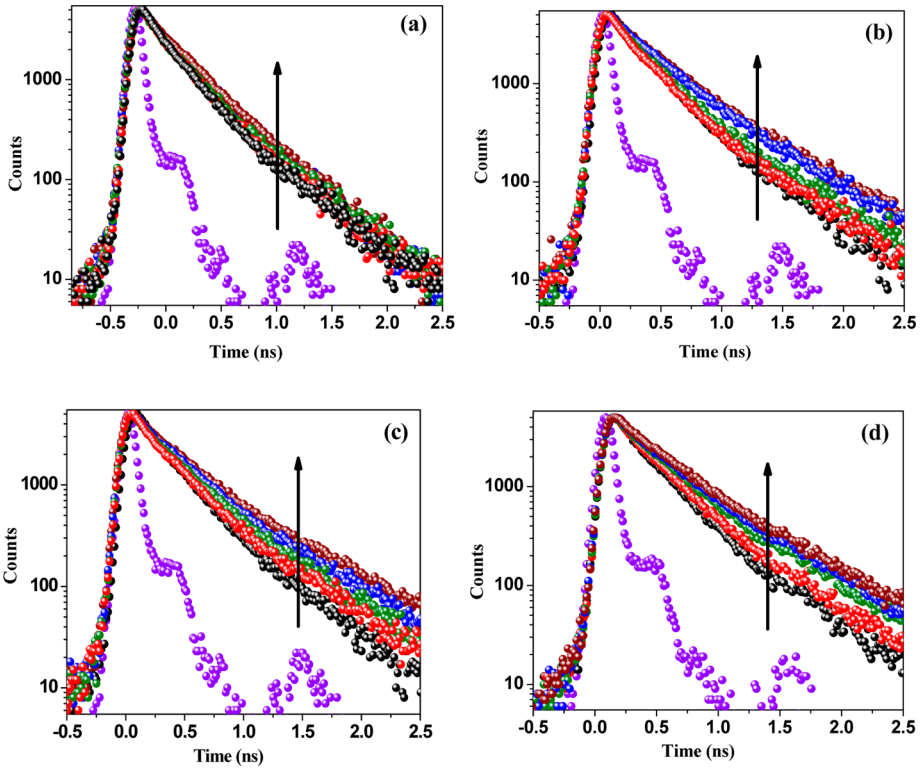

Figure 7. Time-resolved decays of curcumin at W_0 = 0.0, 0.5, 1.0, 1.5, and 2.0 for (a) water/AOT reverse micelle, (b) EG/AOT reverse micelle, (c) GY/AOT reverse micelle, and (d) DMF/AOT reverse micelle.

Table 3. Fluorescence Lifetime, Quantum Yield, and Radiative and Nonradiative Rate Constants of Curcumin with Variation of W_0 Monitored at 485 nm (Lower Energy Emission Peak)

system	W_0	$\tau_1(a_1)$ (ps)	$\tau_2(a_2)$ (ps)	$\langle\tau\rangle$[a] (ps)	quantum yield (ϕ_f)	K_{nr} (s^{-1}) /10^9	K_r (s^{-1})/ 10^8
water/AOT	0	113(0.71)	119(0.29)	232	0.108	3.83	4.65
	0.5	109(0.71)	120(0.29)	229	0.118	3.85	5.15
	1.0	168(0.70)	453(0.30)	253	0.132	3.43	5.21
	1.5	127(0.44)	392(0.56)	275	0.134	3.15	4.87
	2.0	131(0.43)	376(0.57)	270	0.123	3.24	4.55
EG/AOT	0.5	180(0.80)	495(0.20)	243	0.114	3.64	4.70
	1.0	190(0.78)	529(0.22)	265	0.152	3.20	5.73
	1.5	227(0.71)	589(0.29)	332	0.182	2.46	5.48
	2.0	247(0.73)	637(0.27)	352	0.198	2.27	5.62
GY/AOT	0.5	190(0.80)	549(0.20)	262	0.105	3.41	4.00
	1.0	207(0.76)	581(0.24)	297	0.120	2.96	4.04
	1.5	228(0.76)	646(0.24)	328	0.138	2.62	4.20
	2.0	248(0.75)	708(0.25)	363	0.146	2.35	4.02
DMF/AOT	0.5	203(0.80)	530(0.20)	252	0.118	3.5	4.68
	1.0	223(0.72)	530(0.28)	324	0.122	2.71	3.76
	1.5	221(0.67)	594(0.33)	344	0.136	2.51	3.95
	2.0	220(0.63)	610(0.37)	364	0.138	2.36	3.79

[a]Error in experimental data of ±5%.

dx.doi.org/10.1021/jp401840z | J. Phys. Chem. B XXXX, XXX, XXX−XXX

of the studies, average fluorescence lifetimes (τ_{av}) were only compared where τ_{av} can be expressed by eq 2.

All the studies of curcumin give emphasis on ESIPT, as it is a major photophysical process for deactivation of excited state. This decay component, however, was assigned to different molecular processes, such as solvation[49] and ESIPT[50] in the two studies. More recently, Palit and co-workers studied the dynamics of the excited singlet (S_1) state of curcumin in a wide variety of neat solvents using sub-picosecond time-resolved fluorescence and absorption spectroscopic techniques.[51] In nonpolar solvents, because of the presence of the six-membered hydrogen-bonded chelate ring of the cis−enol form, the ESIPT process is expected to be primarily intramolecular in nature, and based on earlier studies, it should be completed within a few hundreds of femtoseconds.[52,53] However, in the case of polar solvent, like methanol, it was reported that the fluorescence lifetime of curcumin has a dominant component with a time constant of roughly 130 ps.[49,50,54] Hence, the similarity between the time scale of ESIPT and the measured fluorescence lifetime indicates that ESIPT is a major photophysical process in the deactivation of the excited state. The lifetime values of curcumin were detected in AOT reverse micelle with variation of core solvents, and the values are collected at a wavelength of 485 nm (longer wavelength maximum). The decays in all cases were biexponential in nature, and we got considerable change in lifetime values with gradual addition of core solvents (water, EG, GY, and DMF), which confirms the modulations of photophysical character of curcumin when encapsulated in AOT reverse micelle. As we already mentioned, the lifetime of curcumin is shortened mainly due to its fast ESIPT process, so if we are able to decrease the rate of the ESIPT process, the lifetime value of curcumin should be increased. We found that the average lifetime of curcumin in AOT/*n*-heptane reverse micelle was 232 ps at W_0 = 0, which is almost 2 times higher compared with common polar solvents. This high value of the lifetime of curcumin in AOT/*n*-heptane reverse micelle can be explained by considering the intermolecular hydrogen bonding between oxygen of the S−O bonds of AOT and curcumin, which decreases the intramolecular proton transfer rate within the keto−enol group. A similar type of hydrogen bonding is reported in the literature; TX-100 micelle can form strong intermolecular hydrogen bonding between oxygen of the C−O bonds in TX-100 and curcumin.[25] In our previous study, we also showed that a similar type of hydrogen bonding is possible between the anions of ionic liquids and curcumin.[43]

To get a vivid picture of the reverse micelle, we also measured the lifetime of curcumin with gradual addition of core solvents. With gradual addition of water, the average lifetime value of curcumin changes from 232 ps at W_0 = 0.0 to 270 ps at W_0 = 2.0. However, in the case of the other three solvents (EG, GY, DMF), the increments of lifetimes are considerably high. With addition of EG, the average lifetime value of curcumin changes from 232 ps at W_0 = 0.0 to 352 ps at W_0 = 2.0; for GY, it changes to 363 ps, and for DMF, it changes to 364 ps. From the above results, it is clear that the increment of lifetime with addition of core solvent is nearly the same. This may be due to the formation of a hydrogen bond between the keto−enol group of curcumin and core solvents. In the case of DMF, dipole−dipole interaction can also perturb the intramolecular hydrogen bond and slows down the ESIPT process. It is also observed that the effect is less pronounced in the case of water. This may be attributed to the radiationless decay channel associated with the fully solvated ESIPT state of the probe in water. We also monitored the lifetime at a high energy emission peak, i.e., 461 nm. However, as we did not get any important information regarding the ESIPT process, the results are not discussed here. The representative time-resolved fluorescence decay profiles of curcumin are shown in the Supporting Information (Figure S4), and the corresponding lifetime values obtained from the biexponential fitting of the decay are given in Table S3 (Supporting Information).

To further interpret the time-resolved emission decay results and to get a better idea about the modulation in the excited state behavior of curcumin upon encapsulation within the reverse micelle aggregates, we have calculated the radiative and nonradiative decay rate constants using the following equations:

$$K_r = \frac{\phi_f}{\langle \tau \rangle_f} \tag{9}$$

$$K_{nr} = \frac{1}{\langle \tau \rangle_f} - K_r \tag{10}$$

where k_r and k_{nr}, respectively, represent the radiative and nonradiative rate constants. The calculated values are given in Table 3. The radiative and nonradiative processes are accordingly modified with the change in the fluorescence lifetime and hence with the caging of the environment. From Table 3, it is evident that, in AOT/*n*-heptane reverse micelle at W_0 = 0, the nonradiative rate constant of curcumin is 3.83 × 10^9 S^{-1}. In an earlier study, we also observed a similar value for nonradiative rate constants inside a micelle formed by a room temperature ionic liquid.[43] More recently, Das and co-workers observed that the fluorescence properties of curcumin in binary solvent mixtures containing methanol (MeOH) are significantly different than mixtures containing chloroform ($CHCl_3$) or acetonitrile (MeCN), which arises primarily due to the modulation of the nonradiative rates of the pigment.[54] However, in strong hydrogen-bond-donating/accepting solvent like methanol, DMF, and DMSO,[50,55] the nonradiative rate constants are quite close to each other and also similar to the k_{nr} value obtained inside the interfacial region of AOT reverse micelle, supporting our previous assumption that the excited state (S_1) of curcumin is perturbed through the intermolecular hydrogen-bond formation between the AOT headgroup and curcumin. The k_{nr} value is reduced with the addition of core solvents, such as water, EG, GY, and DMF (observation range W_0 = 0−2) in AOT/*n*-heptane reverse micelle aggregates, indicating the perturbation of the ESIPT process.

4. CONCLUSION

In conclusion, the results reported here presented detailed information about the modulation of the photophysical properties of a spectroscopic probe like curcumin, a molecule showing the ESIPT process, in aqueous and nonaqueous AOT reverse micelles. In particular, the remarkable enhancement in fluorescence intensity with a distinct red-shift along with a considerable change in time-resolved spectra dictate the sensitivity of the interaction of curcumin with the various core solvents, which can be attributed to the modulation of the hydrogen bonding network on the excited state of curcumin. Our results show that with the addition of various core solvents the lifetime of curcumin increases, indicating the disturbance of the intramolecular hydrogen bond, leading to the reduced efficiency of the nonradiative deactivation mechanism. We

dx.doi.org/10.1021/jp401840z | J. Phys. Chem. B XXXX, XXX, XXX−XXX

showed here that it is possible to control the curcumin emission by simply changing the AOT reverse micelle interface properties by choosing the appropriate polar solvents. Moreover, these reverse micelle systems can be good models to study such processes that occur with biological molecules embedded in biological membranes.

■ ASSOCIATED CONTENT

Supporting Information

Kamlet−Taft parameters, fluorescence lifetime, quantum yield, $E_T(30)$ plot, and radiative and nonradiative rate constants of curcumin with variation of W_0 monitored at 461 nm (higher energy emission peak). This material is available free of charge via the Internet at http://pubs.acs.org.

■ AUTHOR INFORMATION

Corresponding Author

*E-mail: nilmoni@chem.iitkgp.ernet.in. Phone: +91-3222-283332.

Notes

The authors declare no competing financial interest.

■ ACKNOWLEDGMENTS

N.S. is thankful to Council of Scientific and Industrial Research (CSIR) for a generous research grant. C.B. and J.K. are thankful to UGC and C.G., S.M., and S.G. are thankful to CSIR for their research fellowships.

■ REFERENCES

(1) Sharma, O. Antioxidant Activity of Curcumin and Related Compounds. *Biochem. Pharmacol.* **1976**, *25*, 1811−1812.

(2) Srivastava, K. C.; Bordia, A.; Verma, S. K. Curcumin, a Major Component of Food Spice Turmeric (Curcuma longa) Inhibits Aggregation and Alters Eicosanoid Metabolism in Human Blood Platelets. *Prostaglandins, Leukotrienes Essent. Fatty Acids* **1995**, *52*, 223−227.

(3) Sun, Y. M.; Zhang, H. Y.; Chen, D. Z.; Liu, C. B. Theoretical Elucidation on the Antioxidant Mechanism of Curcumin: a DFT Study. *Org. Lett.* **2002**, *4*, 2909−2911.

(4) Barik, A.; Priyadarsini, K. I.; Mohan, H. Photophysical Studies on Binding of Curcumin to Bovine Serum Albumins. *Photochem. Photobiol.* **2003**, *77*, 597−603.

(5) Lee, S. E.; Campbell, B. C.; Molyneux, R. J.; Hasegawa, S.; Lee, H. S. Inhibitory Effects of Naturally Occurring Compounds on Aflatoxin B(1) Biotransformation. *J. Agric. Food Chem.* **2001**, *49*, 5171−5177.

(6) Shim, J. S.; Kim, J. H.; Cho, H. Y.; Yum, Y. N.; Kim, S. H.; Park, H. J.; Shim, B. S.; Choi, S. H.; Kwon, H. J. Irreversible Inhibition of CD13/Aminopeptidase N by the Antiangiogenic Agent Curcumin. *Chem. Biol.* **2003**, *10*, 695−704.

(7) Flynn, D. L.; Rafferty, M. F.; Boctor, A. M. Inhibition of 5-Hydroxy-eicosatetraenoic Acid (5-HETE) Formation in Intact Human Neutrophils by Naturally-Occurring Diarylheptanoids: Inhibitory Activities of Curcuminoids and Yakuchinones. *Prostaglandins, Leukotrienes Med.* **1986**, *22*, 357−360.

(8) Huang, M. T.; Lysz, T.; Ferraro, T.; Abidi, T. F.; Laskin, J. D.; Conney, A. H. Inhibitory Effects of Curcumin on in Vitro Lipoxygenase and Cyclooxygenase Activities in Mouse Epidermis. *Cancer Res.* **1991**, *51*, 813−819.

(9) Huang, M. T.; Smart, R. C.; Wong, C. Q.; Conney, A. H. Inhibitory Effect of Curcumin, Chlorogenic Acid, Caffeic Acid, and Ferulic Acid on Tumor Promotion in Mouse Skin by 12-O-Tetradecanoylphorbol-13-acetate. *Cancer Res.* **1988**, *48*, 5941−5946.

(10) Wortelboer, H. M.; Usta, M.; van der Velde, A. E.; Boersma, M. G.; Spenkelink, B.; van Zanden, J. J.; Rientjens, I. M. C. M.; van Bladeren, P. J.; Cnubben, N. H. Interplay between MRP Inhibition and Metabolism of MRP Inhibitors: the Case of Curcumin. *Chem. Res. Toxicol.* **2003**, *16*, 1642−1651.

(11) Yang, F.; Lim, G. P.; Begum, A. N.; Ubeda, O. J.; Simmons, M. R.; Ambegaokar, S. S.; Chen, P.; Kayed, R.; Glabe, C. G.; Frautschy, S. A.; Cole, G. M. Curcumin Inhibits Formation of Amyloid Beta Oligomers and Fibrils, Binds Plaques, and Reduces Amyloid in Vivo. *J. Biol. Chem.* **2004**, *280*, 5892−5901.

(12) Egan, M. E.; Pearson, M.; Weiner, S. A.; Rajendarn, V.; Rubin, D.; Glochner-Pagel, J.; Canney, S.; Du, K.; Lukacs, G. L.; Caplan, M. J. Curcumin, a Major Constituent of Turmeric, Corrects Cystic Fibrosis Defects. *Science* **2004**, *304*, 600−602.

(13) Aggrawal, B. B.; Sundaram, C.; Malani, N.; Ichikawa, H. Curcumin: the Indian Solid Gold. *Med. Biol.* **2007**, *595*, 1−75.

(14) Mazumder, A.; Neamati, N.; Sunder, S.; Schulz, J.; Perez, H.; Aich, E.; Pommier, Y. Curcumin Analogs with Altered Potencies Against HIV-1 Integrase as Probes for Biochemical Mechanisms of Drug Action. *J. Med. Chem.* **1997**, *40*, 3057−3063.

(15) Sui, Z.; Salto, R.; Li, J.; Craik, C.; Ortiz de Montellano, P. R. Inhibition of the HIV-1 and HIV-2 Proteases by Curcumin and Curcumin Boron Complexes. *Bioorg. Med. Chem.* **1993**, *1*, 415−422.

(16) Qureshi, S.; Shah, A. H.; Ageel, A. M. Toxicity Studies on Alpinia Galanga and Curcuma Longa. *Planta Med.* **1992**, *58*, 124−127.

(17) Lao, C. D.; Ruffin, M. T.; Normolle, D.; Heath, D. D.; Murray, S. I.; Bailey, J. M.; Boggs, M. E.; Crowell, J.; Rock, C. L.; Brenner, D. E. Dose Escalation of a Curcuminoid Formulation. *Altern. Med.* **2006**, *6*, 10.

(18) Anand, P.; Kunnumakkara, A. B.; Newman, R. A.; Aggarwal, B. B. Bioavailability of Curcumin: Problems and Promises. *Mol. Pharmaceutics* **2007**, *4*, 807−818.

(19) Tonnesen, H. H.; Karlsen, J.; Mostad, A. Structural Studies of Curcuminoids. I. The Crystal Structure of Curcumin. *Acta Chem. Scand., Ser. B* **1982**, *36*, 475−480.

(20) Parimita, S. P.; Ramshankar, Y. V.; Suresh, S.; Guru, R. T. N. Redetermination of Curcumin: (1E,4Z,6E)-5-Hydroxy-1,7-bis(4-hydroxy-3-methoxyphenyl)hepta-1,4,6-trien-3-one. *Acta Crystallogr., Sect. E* **2007**, *63*, o860−o862.

(21) Payton, F.; Sandusky, P.; Alworth, W. L. NMR Study of the Solution Structure of Curcumin. *J. Nat. Prod.* **2007**, 143−146.

(22) Erez, Y.; Presiado, I.; Gepshtein, R.; Huppert, D. Temperature Dependence of the Fluorescence Properties of Curcumin. *J. Phys. Chem. A* **2011**, *115*, 10962−10971.

(23) Erez, Y.; Presiado, I.; Gepshtein, R.; Huppert, D. The Effect of a Mild Base on Curcumin in Methanol and Ethanol. *J. Phys. Chem. A* **2012**, *116*, 2039−2048.

(24) Bisht, S.; Feldmann, G.; Soni, S.; Ravi, R.; Karikar, C.; Maitra, A.; Maitra, A. Polymeric Nanoparticle-Encapsulated Curcumin ("nanocurcumin"): a Novel Strategy for Human Cancer Therapy. *J. Nanobiotechnol.* **2007**, *5*, 3.

(25) Adhikary, R.; Carlson, P. J.; Kee, T. W.; Petrich, J. W. Excited-State Intramolecular Hydrogen Atom Transfer of Curcumin in Surfactant Micelles. *J. Phys. Chem. B* **2010**, *114*, 2997−3004.

(26) Leung, M. H. M.; Colangelo, H.; Kee, T. W. Encapsulation of Curcumin in Cationic Micelles Suppresses Alkaline Hydrolysis. *Langmuir* **2008**, *24*, 5672−5675.

(27) Thangapazham, R. L.; Puri, A.; Tele, S.; Blumenthal, R.; Maheshwari, R. K. Evaluation of a Nanotechnology-Based Carrier for Delivery of Curcumin in Prostate Cancer Cells. *Int. J. Oncol.* **2008**, *32*, 1119−1123.

(28) Sun, Y.; Lee, C.-C.; Hung, W. C.; Chen, F. Y.; Lee, M. T.; Huang, H. W. The Bound States of Amphipathic Drugs in Lipid Bilayers: Study of Curcumin. *Biophys. J.* **2008**, *95*, 2318−2324.

(29) Barik, A.; Mishra, B.; Kunwar, A.; Priyadarsini, K. I. Interaction of Curcumin with Human Serum Albumin: Thermodynamic Properties, Fluorescence Energy Transfer and Denaturation Effects. *Chem. Phys. Lett.* **2007**, *436*, 239−243.

(30) Kornherr, A.; Vogtenhuber, D.; Ruckenbauer, M.; Podloucky, R.; Zifferer, G. Multilayer Adsorption of Water at a Rutile TiO2)(110) Surface: Towards a Realistic Modeling by Molecular Dynamics. *J. Chem. Phys.* **2004**, *121*, 3722−3727.

(31) Nandi, N.; Bhattacharyya, K.; Bagchi, B. Dielectric Relaxation and Solvation Dynamics of Water in Complex Chemical and Biological Systems. *Chem. Rev.* **2000**, *100*, 2013−2046.
(32) Bhattacharyya, K. Solvation Dynamics and Proton Transfer in Supramolecular Assemblies. *Acc. Chem. Res.* **2003**, *36*, 95−101.
(33) Pileni, M. P.; Zemb, T.; Petit, C. Solubilization by Reverse Micelles: Solute Localization and Structure Perturbation. *Chem. Phys. Lett.* **1985**, *118*, 414−420.
(34) Pileni, M. P.; Brochette, P.; Hickel, B.; Lerebours, B. Hydrated Electrons in Reverse Micelles: 2 Quenching of Hydrated Electron by Sodium Nitrate. *J. Colloid Interface Sci.* **1984**, *98*, 549−554.
(35) Pileni, M. P. Reverse Micelles as Microreactors. *J. Phys. Chem.* **1993**, *97*, 6961−6973.
(36) Darío Falcone, R.; Correa, N. M.; Biasutti, M. A.; Silber, J. J. Properties of AOT Aqueous and Nonaqueous Microemulsions Sensed by Optical Molecular Probes. *Langmuir* **2000**, *16*, 3070−3076.
(37) Ghatak, C.; Rao, V. G.; Pramanik, R.; Sarkar, S.; Sarkar, N. Nanocavity Effect on Photophysical Properties of Colchicine: a Proof by Circular Dichroism Study and Picosecond Time-Resolved Analysis in Various Reverse Micellar Assemblies. *J. Phys. Chem. B* **2011**, *115*, 6644−6652.
(38) Khopde, S. M.; Priyadarsini, K. I.; Palit, D. K.; Mukherjee, T. Effect of Solvent on the Excited-State Photophysical Properties of Curcumin. *Photochem. Photobiol.* **2000**, *72*, 625−631.
(39) Lakowicz, J. R. *Principles of Fluorescence Spectroscopy*; Plenum: New York, 1999; Vol. *2*.
(40) Chakraborty, A.; Chakrabarty, D.; Hazra, P.; Seth, D.; Sarkar, N. Photoinduced Intermolecular Electron Transfer Between Coumarin Dyes and Electron Donating Solvents in Cetyltrimethylammonium Bromide (CTAB) Micelles: Evidence for Marcus Inverted Region. *Chem. Phys. Lett.* **2003**, *382*, 508−517.
(41) Perez-Casas, S.; Castillo, R.; Costas, M. Effect of Alcohols in AOT Reverse Micelles. A Heat Capacity and Light Scattering Study. *J. Phys. Chem. B* **1997**, *101*, 7043−7054.
(42) Laia, C. A. T.; Lopez-Cornejo, P.; Costa, S. M. B.; d'Oliveira, J.; Martinho, J. M. G. Dynamic Light Scattering Study of AOT Microemulsions with Nonaqueous Polar Additives in an Oil Continuous Phase. *Langmuir* **1998**, *14*, 3531−3537.
(43) Ghatak, C.; Rao, V. G.; Mandal, S.; Ghosh, S.; Sarkar, N. An Understanding of the Modulation of Photophysical Properties of Curcumin Inside a Micelle Formed by an Ionic liquid: a New Possibility of Tunable Drug Delivery System. *J. Phys. Chem. B* **2012**, *116*, 3369−3379.
(44) Falcone, R. D.; Biasutti, M. A.; Correa, N. M.; Silber, J. J.; Lissi, E.; Abuin, E. Effect of the Addition of a Nonaqueous Polar Solvent (Glycerol) on Enzymatic Catalysis in Reverse Micelles. Hydrolysis of 2-Naphthyl Acetate by Alpha-Chymotrypsin. *Langmuir* **2004**, *20*, 5732−5737.
(45) Lissi, E.; Engel, T. Incorporation of n-Alkanols in Reverse Micelles in the AOT/n-Heptane/Water System. *Langmuir* **1992**, *8*, 452−455.
(46) Novaira, M.; Moyano, F.; Biasutti, M. A.; Silber, J. J.; Correa, N. M. An Example of How to Use AOT Reverse Micelle Interfaces to Control a Photoinduced Intramolecular Charge-Transfer Process. *Langmuir* **2008**, *24*, 4637−4646.
(47) *Solubilization in Surfactant Aggregates*; Christian, S. D., Scamehorn, J. F., Eds.; Marcel Decker, Inc.: New York, 1995.
(48) Barltrop, J. A.; Coyle, J. D. *Principles of Photochemistry*; Wiley & Sons: New York, 1978.
(49) Nardo, L.; Paderno, R.; Andreoni, A.; Masson, M.; Haukvik, T.; Tonnesen, H. H. Role of H-Bond Formation in the Photoreactivity of Curcumin. *Spectroscopy* **2008**, *22*, 187−198.
(50) Khopde, S. M.; Priyadarsini, K. I.; Palit, D. K.; Mukherjee, T. Effect of Solvent on the Excited-State Photophysical Properties of Curcumin. *Photochem. Photobiol.* **2000**, *72*, 625−631.
(51) Ghosh, R.; Mondal, J. A.; Palit, D. K. Ultrafast Dynamics of the Excited States of Curcumin in Solution. *J. Phys. Chem. B* **2010**, *114*, 12129−12143.
(52) Schwartz, B. J.; Peteanu, L. A.; Harris, C. B. Direct Observation of Fast Proton Transfer: Femtosecond Photophysics of 3-Hydroxyflavone. *J. Phys. Chem.* **1992**, *96*, 3591−3598.
(53) Arthen-Engeland, Th.; Bultmann, T.; Ernsting, N. P.; Rodriguez, M. A.; Thiel, W. Singlet Excited-State Intramolecular Proton Tranfer in 2-(2t′-Hydroxyphenyl) Benzoxazole: Spectroscopy at Low Temperatures, Femtosecond Transient Absorption, and MNDO Calculations. *Chem. Phys.* **1992**, *163*, 43−53.
(54) Saini, R. K.; Das, K. Picosecond Spectral Relaxation of Curcumin Excited State in a Binary Solvent Mixture of Toluene and Methanol. *J. Phys. Chem. B* **2012**, *116*, 10357−10363.
(55) Chignell, C. F.; Bilski, P.; Reszka, K. J.; Motten, A. N.; Sik, R. H.; Dhal, T. A. Spectral and Photochemical Properties of Curcumin. *Photochem. Photobiol.* **1994**, *59*, 295−302.